

A Process Model for Underground Coal Gasification: Part-II

Growth of Outflow Channel

(Preprint version of an original research article to be submitted to Fuel Journal)



Indian Institute of Technology Bombay

A Process Model for Underground Coal Gasification: Part-II

Growth of Outflow Channel

Ganesh Samdani¹, Preeti Aghalayam², Anuradda Ganesh³, R. K. Sapru⁴, B. L. Lohar⁴
and Sanjay Mahajani^{*,1}

¹Department of Chemical Engineering, Indian Institute of Technology Bombay, Powai, Mumbai 400076

²Department of Chemical Engineering, Indian Institute of Technology Madras, Chennai 600036

³Department of Energy Science and Engineering, Indian Institute of Technology Bombay, Powai, Mumbai 400076

⁴Institute of Reservoir Studies, ONGC, Ahmedabad

Abstract

Underground Coal Gasification is a process of gasifying coal *in-situ* to produce syn-gas. The gas thus produced, passes through the outflow channel that leads to the production well. As explained in part-I of this paper (Samdani et al., 2014), cavity growth between injection and production wells happens in two distinct phases. This paper presents an unsteady state model for cavity growth and gas production in phase-II wherein, the growth occurs mostly in horizontal direction towards the production well through the outflow channel. This phase of UCG lasts much longer than phase-I, in which growth takes place in vertical direction till the cavity hits the overburden. In the model for phase-II, the outflow channel is divided in small sections along its length and each section includes three subzones i.e. rubble zone, void zone and roof at the top. A compartment model is developed to reduce the complexity caused by non-ideal flow patterns and changing sizes of different subzones inside the outflow channel. The subzones and the sections are linked appropriately, for mass and energy flow, to give overall performance during Phase-II of UCG. The proposed approach combines chemical reactions, heat and mass transfer effects, spalling characteristic and complex flow patterns to achieve meaningful results. In all, seven gas species, three solid species and eleven reactions are included. The simulation results such as variation in solid density, dynamics of different zones, exit gas quality are presented. The model is validated by comparing the predicted exit gas quality and that observed during similar laboratory scale experiments. Finally the results are also compared with field scale experiments. This model along with the Phase-I model provides a complete modeling solution for UCG process.

Keywords: Underground coal gasification, outflow channel, compartment model, spalling

*Corresponding author. Tel.: +91 (0) 22 25767246. E-mail address: sanjaym@iitb.ac.in

Introduction

Underground coal gasification (UCG) is a process of producing syn-gas by gasifying coal in-situ that is otherwise technically or economically unminable¹. The process involves a sequence of steps starting from drilling of injection and production wells to the syngas generation, by injecting gasifying agents. Figure 1 shows the typical steps involved in UCG process and different phases of UCG, as explained in our previous work².

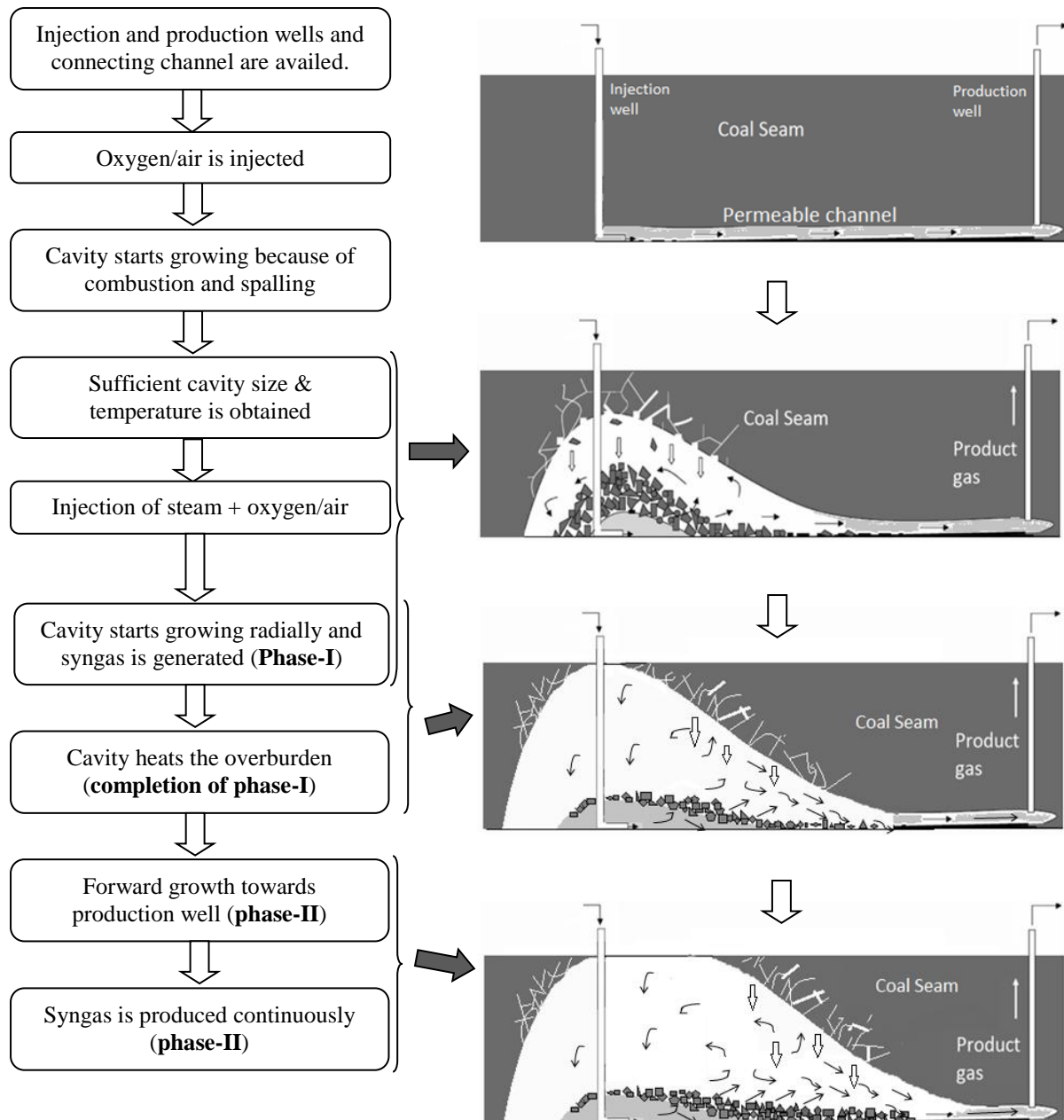


Figure 1. Schematic of UCG showing different phases of UCG cavity growth²

The injection and production wells are typically around 50-60 m apart from each other³. This distance depends on available reserves, permeability and thickness of coal seam. The cavity

near the injection well starts growing initially and it reaches the overburden much earlier compared to reaching the production well. This is because of the longer distance between injection and production wells compared to coal seam thickness. After the cavity hits the overburden, growth starts in lateral direction towards the production well. This phase of lateral growth is termed as Phase-II, which is essentially the gasification happening in outflow channel. Since the outflow channel is considerably long, this phase of UCG lasts much longer than the previous one. The outflow channel, in the absence of spalling, can be modeled like a channel gasifier with reactive porous walls. However, in case of coal with a tendency to spall, underground gasifier geometry becomes complex due to the presence of rubble on the floor of outflow channel as well. There have been several studies reported in literature to model channel gasifiers⁴⁻¹⁰. These studies either do not consider complex flow patterns and spalling, or oversimplify their presence. A notable effort by Chang⁵ is on developing a process model for channel gasifier, which is partially filled by spalled rubble; however their definition of spalling is not mechanistic and it needs estimation of three empirical constants for every coal. Their model also assumes equilibrium for water-gas-shift reaction. Later few other researchers^{11,12} also attempted to model spalling which was limited by dimensionality of model or approximate spalling definitions. In view of the previous models, it can be said that there is no work which considers UCG in two distinct phases and models the complex reaction chemistry, flow dynamics and spalling, all at a time.

In the present work, we propose a modeling strategy for gasification in Phase-II of UCG and predict the UCG performance for a lignite reserve from Vastan, Surat, India. Both, this model and the Phase-I model presented earlier², can be conveniently used for other coals as well, provided that the data on kinetics and spalling for the respective coals are available. Compartment modelling approach, based on reported RTD studies for actual field trials, is used to describe gasification in Phase-II i.e. for the growth in forward direction. This is accomplished by developing an unsteady state model for different zones in the outflow channel.

Model development for UCG during Phase-II: growth of outflow channel

To develop a model for UCG, different inputs like kinetics, heat and mass transfer correlations, spalling characteristics, flow patterns etc. are required. These inputs and their importance in a UCG model have already been detailed in Part-I of the paper.

Figure 2 shows a typical shape of UCG cavity at the end of phase-I, which essentially is cavity followed by the outflow channel. At any given time, spalled rubble is present only till some distance from the injection well, as the extent of spalling is less in the outflow channel due to lower temperature and lower degree of pyrolysis of coal seam prevailing in that region.

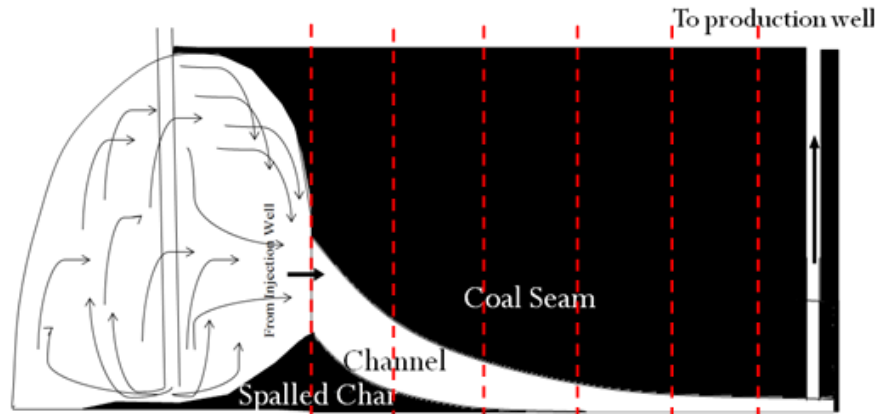


Figure 2. Schematic of outflow channel of UCG cavity (Phase-II)

Several RTD studies have been performed in UCG field trials¹³⁻¹⁴. The tracer studies for Hoe Creek-II show the presence of two gasification paths because of the existence of both void space and rubble for at least some part of the outflow channel. However, a modified single-path tanks-in-series model is used for simulating the UCG outflow channel as the loss of representativeness is relatively minor⁵. These tanks divide the outflow channel into sections along the distance between the injection and production wells (Figure 2). Each section is termed as a compartment and one such compartment with detailed interaction between its different zones and other compartments is shown in Figure 3a.

Each compartment consists of void in channel, rubble (consisting of coal, char and ash) on the floor of channel and dry and wet zones inside the roof. The shape of the outflow channel is assumed to be half-cylinder with cylinder axis along the length of channel and the channel diameter reducing towards the production well. To accommodate two paths in the channel, the inlet stream to a compartment splits into parts: one entering the void and the other passing through the rubble. These two streams are of same composition but different flow rates and the distribution of flow between void and rubble is assumed to be proportional to the empty (porous) volume in void and rubble zone. Further at the exit of any compartment, streams from both rubble and void get mixed and later the mixed stream splits again into two streams of different flow rates.

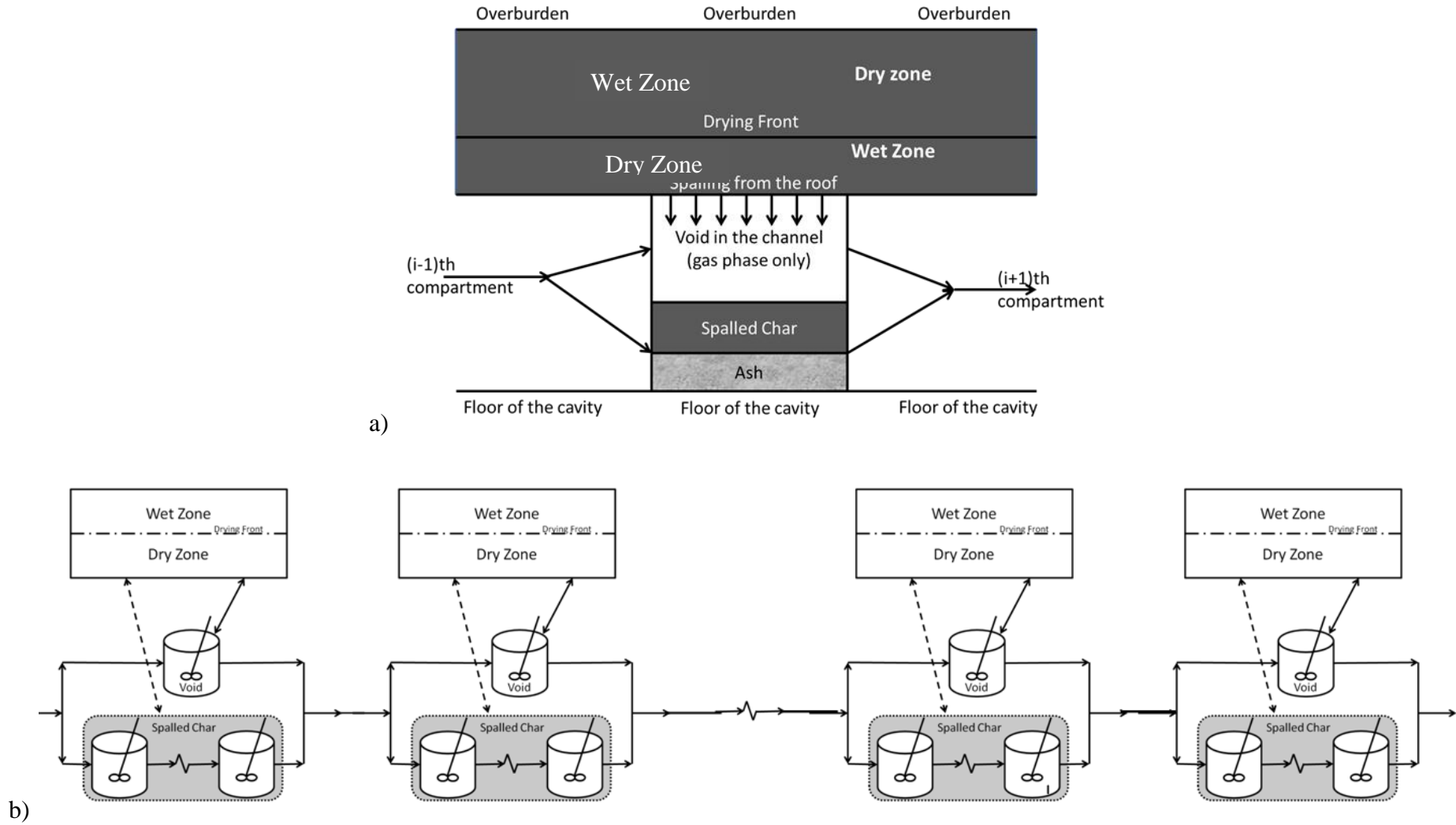


Figure 3. Schematic of a) compartment and b) proposed model for outflow channel modeling

This mixing and splitting of gas streams after every compartment facilitates the redistribution of gases based on porous volumes of different zones in any compartment. Heat is transferred by convection between rubble and void; and by radiation between rubble and the roof in each compartment.

It is assumed that the gas flow is completely mixed in the void zone of any compartment. The extent of axial mixing for the flow in the rubble zone is however assumed to be relatively less and is represented by CSTRs in series. Basis for this observation is that when the gases have to flow through porous solids, there is a resistance for axial mixing in rubble, whereas empty void zone shows higher axial mixing. The above observation is for void zone in one compartment only. Overall, a series of CSTRs represents the total void in the channel, as the channel is divided in compartments of different sizes. On the other hand, diffusion is assumed to be the only mode of species transport inside the coal seam above the void. As the size of rubble zone in the channel varies from inlet to outlet, the number and sizes of mixed flow reactors representing the rubble zone may also vary. Similarly, the size of mixed flow reactor representing void in a compartment also decreases from the inlet end to the outlet end. At a given time, after some distance from the inlet, the size of permeable channel remains constant, as it is unaffected by the upstream processes. Figure 3b provides a generalized reactor network proposed for modeling of phase-II of UCG. The exact number of compartments in the channel and mixed flow reactors in the rubble may be determined by performing detailed residence time distribution studies on the outflow channel geometry for a given coal. In this work, a single mixed flow reactor is assumed to represent the rubble zone. In the following section, the models of different zones in each compartment are described along with the assumptions and important features.

Rubble zone model for spalled char/coal

As mentioned earlier, rubble zone in every compartment is modeled as a single CSTR. The important characteristic of this CSTR model is that there are no spatial variations of temperature and gas phase composition inside the entire rubble in a compartment.

The various other assumptions and important features of the model are as follows:

- Mass and energy balances are written separately for the solid and the gas species.
- Complete mixing takes place throughout the rubble zone in a compartment causing

uniform temperature and compositions of the solid and gas phases everywhere.

- Gas phase consists of seven species N₂, O₂, H₂O, H₂, CH₄, CO and CO₂. Nitrogen is not present if pure oxygen is injected.
- Solid phase consists of three species: coal, char and ash.
- A set of ten reactions is considered: pyrolysis, spontaneous reforming of tar, four char reactions, water gas shift reaction and three gas phase oxidation reactions.
- Drying is not considered in the rubble zone as the spalled coal is completely dried before it spalls from the roof.
- Solid and gas phase temperatures are directly affected by heterogeneous and homogeneous reactions, respectively, and are related through a suitable correlation for the convective heat-transfer coefficient.
- Heat is transferred to the roof by radiation from the external top surface of the rubble.
- The mass transfer resistance at the gas-solid interface is considered for of all the heterogeneous reactions.
- No volume contraction is considered because of reaction, however, rubble volume increases because of spalling from roof.

Gas phase species mass balance

$$\frac{\partial C_{gi}}{\partial t} = \frac{1}{\tau_{spall}} \left(C_{gi,in} - C_{gi} \frac{v}{v_{in}} \right) + \sum_{j=1}^n a_{ij} R_j \quad (1)$$

Initial condition: at t = 0, C_{gi} = C_{gi,0}

Gas phase energy balance

$$\sum_{i=1}^n C_{gi} C_{pi} \frac{\partial T_g}{\partial t} = \frac{1}{\tau} \left(C_{gi,in} H_{i,in} - C_{gi} H_i \frac{v}{v_{in}} \right) - h_T (T_g - T_s) - \sum_{j=1}^n \Delta H_j R_j \quad (2)$$

Boundary condition: at t = 0, T_g = T_{g,0}

Gas phase volumetric flow rate

$$\frac{v}{v_0} = \frac{(\tau_{spall} \sum_i \sum_{j=1}^n a_{ij} R_j M_i + \sum_i C_{gi,in} M_i)}{\sum_i C_{gi} M_i} \quad (3)$$

Here, $\tau_{spall} = \frac{V_{spall}}{v_0}$ and v is volumetric flow rate of exit gas from rubble.

Solid phase species mass balance

$$\frac{\partial \rho_i}{\partial t} = M_i \sum_{j=1}^n a_{s,ij} R_j \quad (4)$$

Initial condition: at $t = 0$; $\rho_i = \rho_{i,0}$

Solid phase energy balance

$$\sum_i \rho_i C_{ps,i} \frac{\partial T_s}{\partial t} = h_T (T_g - T_s) - \sum_{j=1}^n \Delta H_j R_j - \frac{\sigma \epsilon_r}{2 - \epsilon_r} (T_s^4 - T_{roof}^4) A_{spall} / V_{spall} - h_{T,cav} (T_s - T_{void}) A_{spall} / V_{spall} \quad (5)$$

Initial condition: At $t = 0$, $T_s = T_{s,0}$

The back-mixed reactor model gives rise to stiff ordinary differential equations in time for the solid and gas phase balances.

Back mixed reactor model for the void space in the cavity

This model is similar to the sub-model for void space in the radially growing cavity evolved during Phase-I of the growth. The difference is that the channel is assumed to be a half-cylinder with cross sectional area decreasing towards the production well. The radius of the channel near the injection well is of the order the height of coal seam. The assumptions used for developing this model can be found in part-I of this paper². and the model equations are provided here by equations 6-8 below.

Gas species mass balance

$$\frac{\partial C_{gi}}{\partial t} = \frac{1}{\tau_{void}} \left(C_{gi,in} - C_{gi} \frac{v}{v_{in}} \right) + \sum_{j=1}^n a_{ij} R_j + k_{y,cav} (C_{gi,roof} - C_{gi}) A_{roof} / V_{cav} \quad (6)$$

Initial value: at $t = 0$, $C_{gi} = C_{gi,0}$

Gas phase energy balance

$$\sum_{i=1}^n C_{gi} C_{pi} \frac{\partial T_g}{\partial t} = \frac{1}{\tau} \left(C_{gi,in} H_{i,in} - C_{gi} H_i \frac{v}{v_{in}} \right) - \sum_{j=1}^n \Delta H_j R_j - F_w \Delta H_{vap} + k_{y,cav} (C_{gi,roof} - C_{gi}) H_{i,roof} A_{roof} / V_{cav} + h_{T,cav} (T_{s,roof} - T_g) A_{roof} / V_{cav} + h_{T,cav} (T_{s,spall} - T_g) A_{spall} / V_{spall} \quad (7)$$

Boundary condition: at $t = 0$, $T_g = T_{g,0}$

Gas phase volumetric flow rate

$$\frac{v}{v_0} = \frac{(\tau_{void} \sum_i \sum_{j=1}^n a_{ij} R_j M_i + \sum_i C_{gi,in} M_i)}{\sum_i C_{gi} M_i} \quad (8)$$

Here, $\tau_{void} = \frac{V_{void}}{v_0}$ and v is volumetric flow rate of exit gas from void.

Roof model for coal seam above the void

The sub-model for roof is also similar to the one presented earlier for modeling the roof during Phase-I of cavity growth². Details of the assumptions considered for developing this model can be found in part-I of this paper².

The mathematical equations describing the roof model are divided in two parts i.e. dry zone and wet zone.

Dry zone

In dry zone, the balance equations for temperature, mass flux, gas species, and solid densities are solved with appropriate boundary conditions. Heat transfer to the roof of a compartment is by convection from the void as well as by radiation from the top external surface of the rubble in that compartment. It is also assumed that ash falls apart instantaneously from the char surface.

Solid phase balance

$$\frac{\partial \rho_i}{\partial t} = M_i \sum_{j=1}^n a_{s,ij} R_j \quad (9)$$

Initial condition: at $t = 0$; $\rho_i = \rho_{i,0}$

The dry zone model assumes that the gas and the solid phases are in thermal equilibrium and thus only one heat balance equation is solved. The boundary conditions for the energy balance equation are: constant temperature at drying front and, radiation and convection at the boundary open to the cavity.

$$\sum_i \rho_i C_{ps,i} \frac{\partial T_s}{\partial t} = \frac{\partial}{\partial v} \left[k_{eff} A_c^2 \frac{\partial T_s}{\partial v} \right] - \sum_{j=1}^n \Delta H_j R_j \quad (10)$$

Initial condition: at $t = 0$, $T_s = T_{s,0}$

Boundary conditions: at $V = V_d$, $T_s = T_d$

$$\text{at } V = V_0, -k_{eff}A_{roof} \frac{\partial T_s}{\partial V} = \frac{\sigma \varepsilon_r}{2 - \varepsilon_r} (T_{s,spall}^4 - T_s^4) + h_{T,cav}(T_{void} - T_s)$$

Gas phase balance

Because of the large differences in characteristic times of solid and gas phase variation, we assume pseudo-state for gas species balance.

$$\frac{\partial}{\partial V} \left[D_{eff} A_c^2 \frac{\partial C_{gi}}{\partial V} \right] + \sum_{j=1}^n a_{ij} R_j = 0 \quad (11)$$

Convective boundary condition is used at the void side end of the roof; and gas species flux at the drying front is zero for all gases except steam. Steam flux is later related to velocity of drying front.

$$\text{at } V = V_{roof}, -D_{eff} A_{roof} \frac{\partial C_{gi}}{\partial V} = k_{y,cav} (C_{gi,void} - C_{gi,roof})$$

$$\text{at } V = V_d, -D_{eff} A_d \frac{\partial C_{gi}}{\partial V} = 0; \text{ and } -D_{eff} A_d \frac{\partial C_{steam}}{\partial V} = v_{df} \phi (\rho_{w,l} - \rho_{w,g}) / M_w$$

Where, v_{df} is velocity of drying front, calculated later in this section.

Wet zone

Due to uniform moisture content everywhere in wet zone and no reactions occurring, only a heat balance equation needs to be defined for wet zone with conduction as the only mode of heat transfer.

$$\rho_s C_{ps} \frac{\partial T_s}{\partial t} = \frac{\partial}{\partial V} \left[k A_c^2 \frac{\partial T_s}{\partial V} \right] \quad (12)$$

Boundary conditions:

$$\text{at } V = V_T, T_s = T_T \quad \text{and} \quad \text{at } V = V_d, T_s = T_d$$

Drying front

The velocity of the moving front, at which drying takes place, can be calculated from the difference in the heat flux across the drying front (eq. 13). The net heat flux across the drying front, located at x_d , determines the mass flux of steam that enters the dry zone.

$$v_{df} = \frac{1}{\phi(\rho_{w,l} - \rho_{w,g})/M_w} \left(\frac{-k_{d-} \left[\frac{\partial T}{\partial x} \right]_{d-} + k_{d+} \left[\frac{\partial T}{\partial x} \right]_{d+}}{\Delta H_{vap}} \right) \quad (13)$$

Once the drying front velocity is calculated by using eq. 13, increase in the size of dry zone needs to be determined. The different variables corresponding to the newly added nodes in the dry zone are defined as per the scheme designed in part-I of this paper².

Spalling

Spalling is the thermo-mechanical failure of coal/char particles on the floor of the cavity, under the UCG conditions of high temperature and increased porosity of underground coal seam. Spalling is advantageous to UCG as it increases available surface area for reactions however it complicates modeling by introducing new parameters in the model and causes changes in the cavity size during the process. Definition of spalling for Phase-I model is based on temperature of top layer of the rubble zone. However, phase-II model considers the rubble as a CSTR, which does not allow us to use same parameters for defining spalling condition. A way out is to convert the spalling conditions from model-I into equivalent roof zone conditions. In this model, rate of spalling is introduced as a function of dry zone dynamics in such a way that the spalling occurs if coal density inside the dry zone reduces below the critical coal density i.e. spalling limit. This limit is a function of the coal properties and its type. In the present work, critical coal density is considered to be 60% of its initial density. Value of critical density directly affects the spalling rate and it is an important parameter.

Apart from spalling, heat and mass transfer correlations and reaction kinetics are other important input parameters for this model. Drying, pyrolysis, different heterogeneous and homogeneous chemical reactions and their kinetic models used in the phase-II model are similar to the ones used in modeling of initial cavity growth². Heat and mass transfer effects are also treated in similar manner.

Solution Procedure

Figure 4 shows the algorithm for solving the model equations for Phase-II of UCG process. The equations are divided in following five sets: dry zone balances, wet zone balances, solid phase balances in rubble zone, gas phase balances in rubble zone and gas phase balances for void zone. Solution procedure starts from the first compartment in the outflow channel by solving for balances in the cavity roof composed of dry and wet zones.

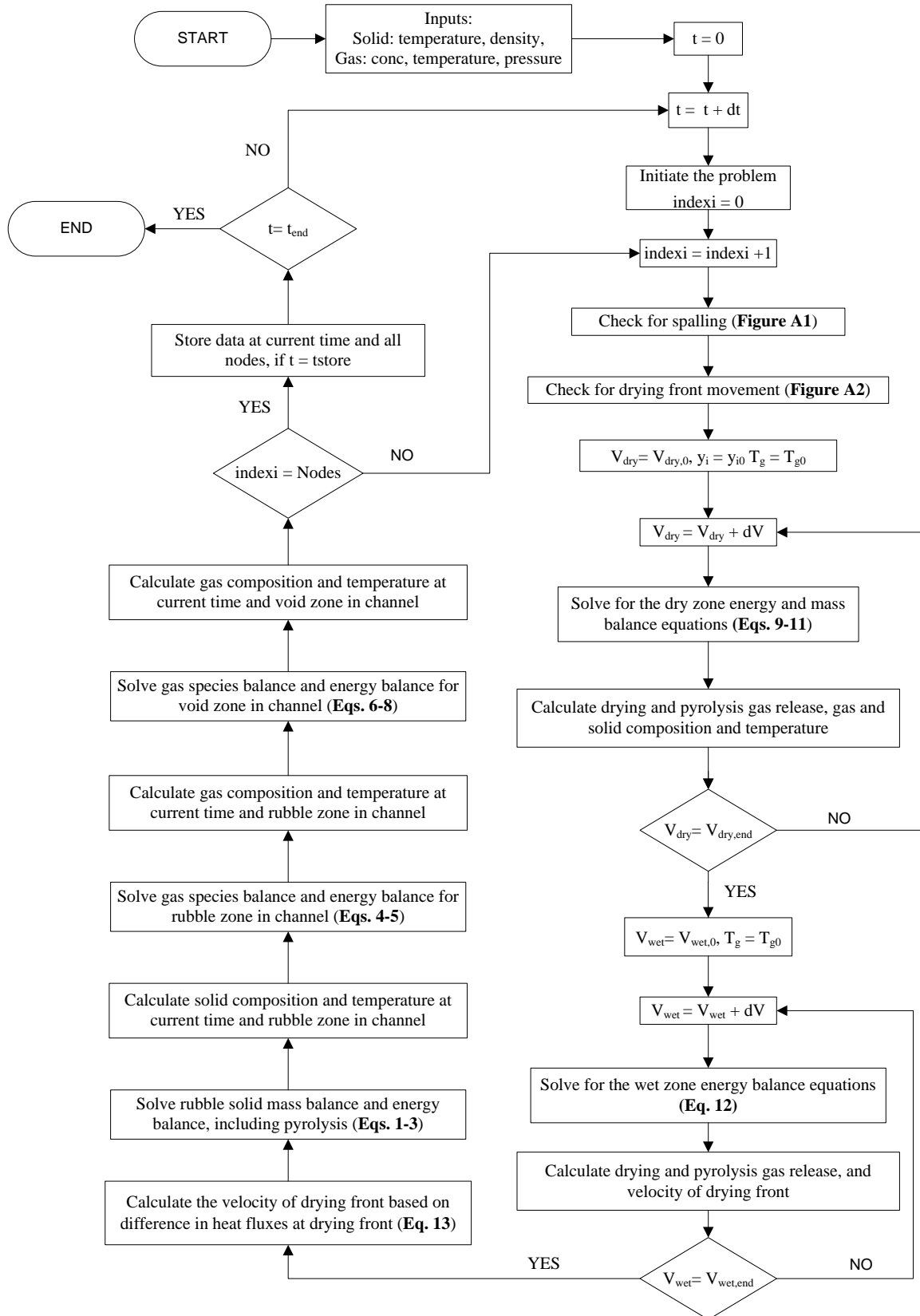


Figure 4. Solution procedure for the model for Phase II of cavity growth

While dry zone model is the set of DAEs, the wet zone model comprises of heat balance equation only. Solution of dry zone and wet zone balance equations are used to calculate the

drying front velocity. Dry zone volume is increased if the cumulative drying front movement is sufficiently high. The solution of roof model also provides the information to check whether spalling condition is satisfied. Later, the rubble zone model is solved. The model comprises of two sets of ODEs *viz.* solid phase balance equations and gas phase balance equations. Finally, the void zone balance equations for gas phase species and energy are solved simultaneously. This procedure is repeated till the last compartment before moving to the next time interval. Estimates for the solution at any time level in any compartment are made based on the solutions at the previous time level for the same compartment. The above procedure is repeated till the final time.

Results and discussion

Input parameters for the model are either specified earlier in this paper or in part-I of this work². Two other important input parameters which are needed for simulating process model of phase-II of UCG. They are total number of compartments in the outflow channel, and the length of each compartment; the values considered are 10 and 0.5m respectively. The size of compartment changes only because of decreasing radius of hemi cylindrical channel. The model is the complex network of ideal reactors and hence the interpretation of the results is not straightforward. For example, if spalling takes place in i^{th} compartment, gas composition and temperatures in all the downstream compartments are influenced.

It is also observed that the product gas mole fraction decreases once the rubble present on the floor of cavity is completely consumed as this reduces the overall reaction rate. Moreover, this causes delay in further spalling as the net exothermic effect caused by the reactions inside the rubble ceases when there is no rubble present on the floor of the channel. In this case, reactions occur only at the roof of the cavity, and the extent of the reactions at the roof is very less for the given values of coal porosities and gas diffusivities. Because of the reduction in the rates of reactions, the exit gas calorific value decreases. Comparison of the exit gas composition profiles for different initial rubble volumes, as shown in figure 5, indicates that the composition of gases improves in case of larger rubble size and the process can be sustained only if sufficiently large amount of rubble is present initially. Therefore a sufficient quantity of rubble is required on the floor of any compartment. In reality, when hot gases produced during phase-I of UCG pass through the outflow channel, they heat the coal at on the wall of the surrounding outflow channel. This can lead to drying, pyrolysis and possible spalling. Therefore, some amount of coal and char can be present on the floor of

outflow channel till some length, even before start of the phase-II. The state of the outflow channel at the start of phase-II is being approximated by the condition of constant non-zero char density till the first spalling instance occurs.

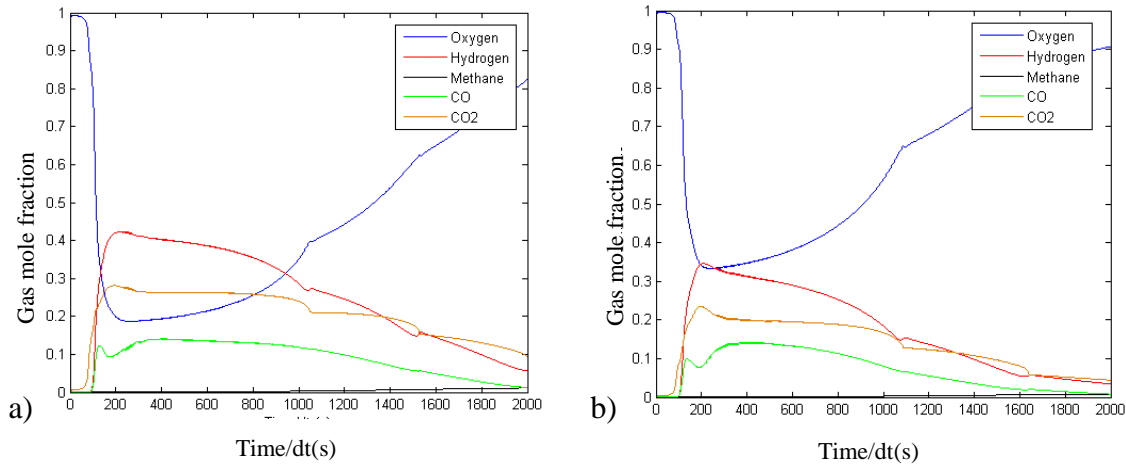


Figure 5 Composition of gases (on dry basis) leaving the channel with spalled char = a) 22 kg and b)14 kg

In the following section of the paper, few of the representative results of the simulation are described. Out of 10 compartments assumed in this study, compartment number 5 is chosen as a representative compartment for interpreting the results. Figure 6a shows the profile of coal density in rubble zone of the compartment-5. Rubble contains only char and no coal before the first spalling instance, as coal is added to the rubble only by spalling. At the spalling instance, density of coal increases in the compartment-5 which later starts reducing because of conversion of coal into char and other pyrolysis products. This decrease in coal density continues till the next spalling instance, which adds more coal to the rubble.

Similarly, the profile of char density in rubble from compartment-5, as shown in figure 6b, can be explained by spalling dynamics. The solid, detached from the roof, contains more coal and less char, which reduces the net density of char in the rubble at every spalling instance. However, char density starts increasing just after this sharp reduction, due to rapid pyrolysis of spalled coal at higher temperatures in the rubble zone. While pyrolysis is taking place, char also gets consumed due to reactions with oxidants and gasifying agents. This leads to a peak in the char density after every instance of spalling. If spalling does not occur before the complete consumption of char in rubble, temperature of gases in rubble reduces to the inlet gas temperature because of the absence of reaction; it is evident between 7-8 hrs of figure 6b. This further delays next spalling. Delay in further spalling can be explained by figure 6c, which is the profile of density of coal at the roof of the channel in compartment-5. Coal density at the roof of the channel reduces because of pyrolysis. Therefore, it can be said that

the observed coal density is related to the degree of pyrolysis which determines rate of spalling in any compartment. As it can be observed in figure 6c, coal density at the roof reduces between any two spalling instances, and it suddenly increases at the spalling instance. This increase in coal density is attributed to the exposure of less-pyrolysed coal from the roof after spalling of coal exposed to the void. In between 7 and 8 hours, the rate of decrease in coal density is reduced and spalling is delayed. The reason for delayed spalling is the non-availability of char in rubble zone after ~7.5 hrs as shown in figure 6b, and this adversely affects the heat transferred to the roof from the rubble.

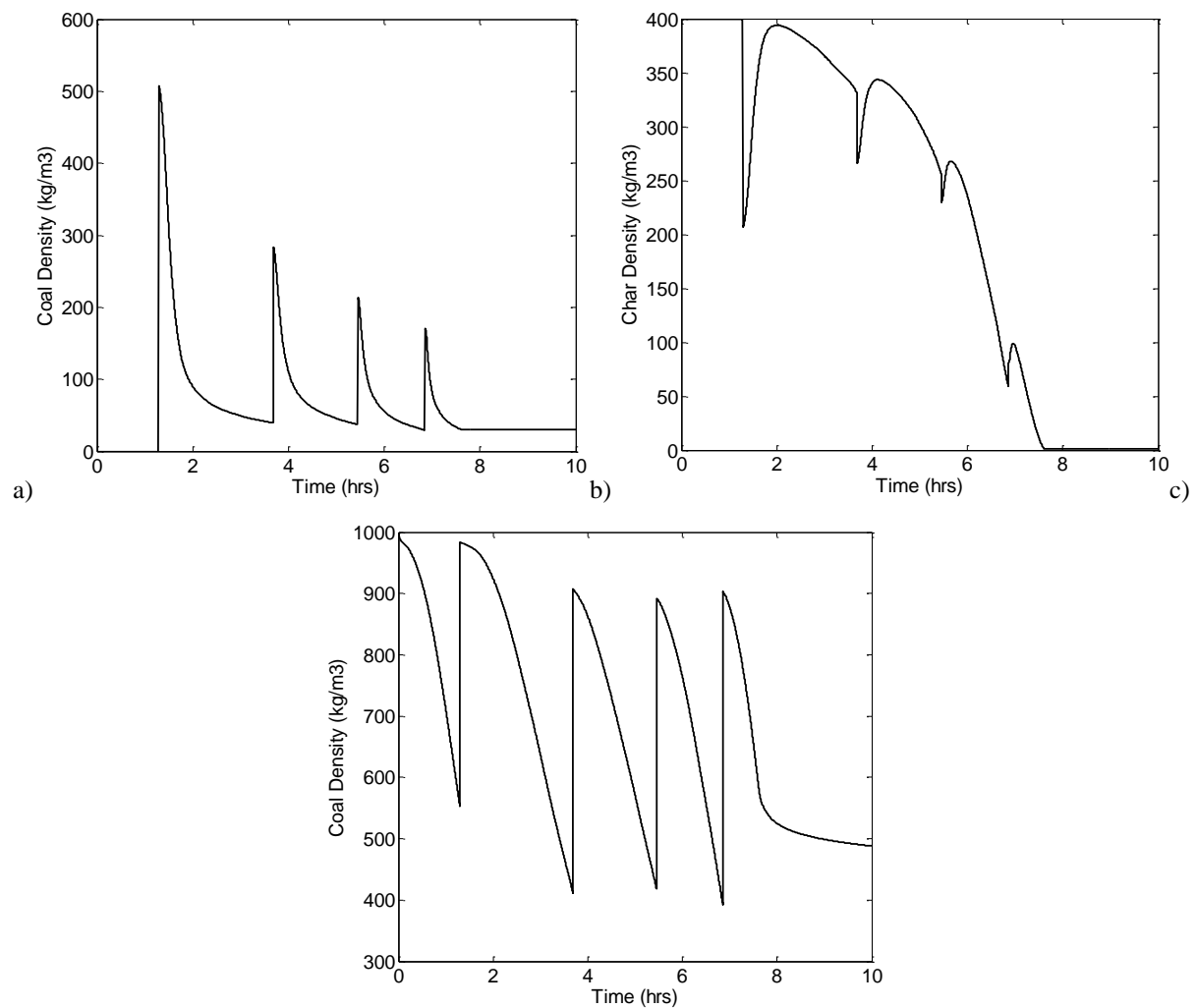


Figure 6. Profile of a) density of coal and b) density of char in rubble zone for compartment-5, c) density of coal at roof surface of compartment-5

Figure 7 shows the plot of mole fractions of the gas species along the length of outflow channel after 6 hrs. Oxygen and steam remain almost unreacted till a distance of 1.5 m from the entry point, indicating absence of coal till this distance. After this point in the channel, a compartment with substantial amount of char in its rubble is present i.e. reaction front. Once

the reactants reach the reaction front, oxygen starts reacting exothermically, which triggers gasification reactions to produce CO and H₂. We observe a continuous increase in hydrogen and carbon dioxide mole fractions while carbon monoxide and steam compositions decrease along the length of channel. This is because of the reversible water-gas shift reaction taking place in all the compartments ahead of reaction front. As methanation is slow due to low pressure, methane is present in very small fractions at any point in the channel.

Error! Reference source not found.a shows the composition profiles of the gases leaving the outflow channel (on dry basis) against time. Due to combustion reaction oxygen gets consumed very rapidly in the rubble zone but part of it also bypasses through the void in the channel. It is also observed that the average composition of product gas remains constant for a long duration. The fluctuations in the composition are because of instances of spalling in different compartments. Total 37 spalling instances are observed in the given time for all the compartments put together, which is exactly equal to the number of fluctuations in the outlet gas composition and hence in the calorific value. The fluctuations at the spalling instances are because of change in WGS reaction equilibrium and fast pyrolysis of coal after it spalls. It can also be observed from the profiles that the oxygen mole fraction in the exit gas starts increasing after 8 hrs. This is the time when the reaction front has crossed half the channel. At the end (10 hrs), the reaction front reaches ninth compartment of the outflow channel which further increases the oxygen mole fraction in the exit gas.

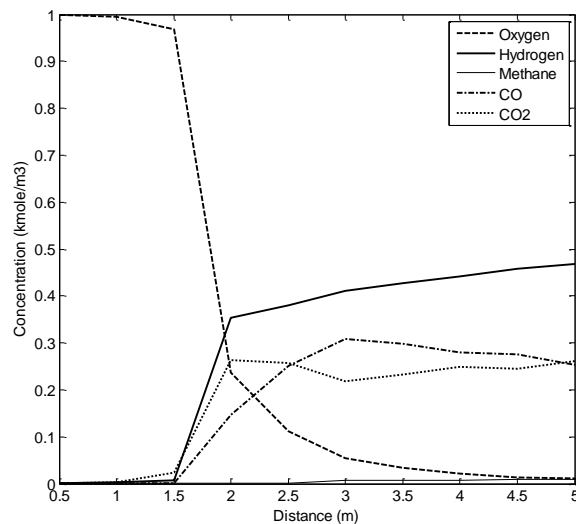


Figure 7. Composition of gases along the length of outflow channel after 6 hrs

Figure 8b shows the variation in calorific value (CV) of the exit gas (on dry basis) from the outflow channel. The exit gas CV is calculated as:

$$\text{Calorific value (kJ/mol)} = H_{\text{CO}} y_{\text{CO}} + H_{\text{H}_2} y_{\text{H}_2} + H_{\text{CH}_4} y_{\text{CH}_4} \quad (14)$$

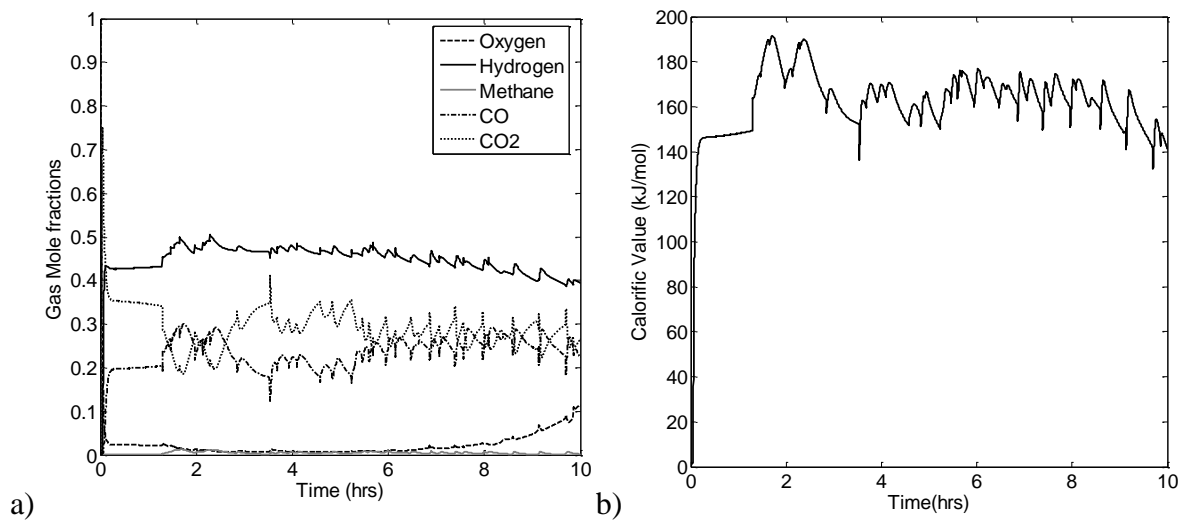


Figure 8 Profile of a) composition of gases leaving the channel, b) calorific value of exit gas

Calorific value of the exit gas fluctuates around a fairly constant value. The reason for the constant average CV is the availability of sufficient coal/char in the compartments beyond the reaction front. As the reaction front moves further, at some time, part of inlet oxygen starts appearing in the exit gas. This also affects the calorific value and therefore it starts reducing after ~8 hrs. The time after which the average calorific value decreases, depends obviously on the distance between entry and exit points i.e. injection and production wells.

Comparison with laboratory scale experiments

This process model has been used to explain experimental observation during UCG experiments performed earlier to determine spalling effects and criteria¹⁵. For the comparison with lab-scale experiments, the process model developed in this work was appropriately downscaled to the shape and size of the spalling apparatus and the simulations were performed at experimental operating and observed spalling conditions. These experiments were performed on a spalling apparatus which mimics the flow conditions in actual outflow channel. More details of these experiments and the results can be found elsewhere¹⁵. Figure 9 shows that the proposed model is able to predict the product gas calorific values as well as

the time required for the consumption of available coal during a UCG-spalling experiment.

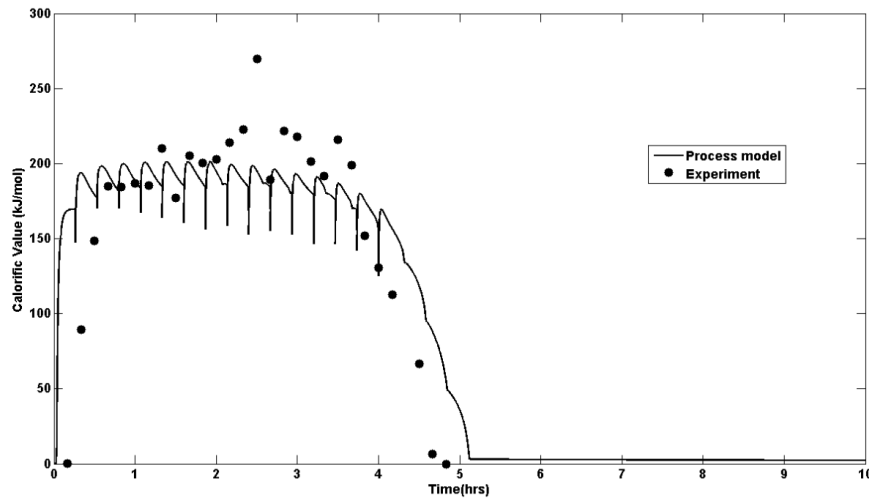


Figure 9. Comparison of experimental and simulation results for product gas calorific value¹⁵

Simulations were also performed at different spalling rates and the average calorific values of product gas at different rates of spalling were observed. It showed that the increase in spalling rate enhances the exit gas calorific value till a certain spalling rate however, it does not have any effect afterwards. This particular spalling rate has been termed as critical spalling rate in our earlier work¹⁶. Above the critical spalling rate, the only limiting factor for char reactions is the availability of reacting gases in the rubble zone.

Comparison of phase-I and phase-II model performance for Vastan Coal Reserve

As it has been reported earlier in this paper, the process model developed for the two phases of UCG is to be used to predict the performance of UCG of Vastan coal mine. The thickness of coal seam of interest is around 6 m and the distance between the injection and production wells may be considered as 40 m. With these dimensions in view, initial cavity size till the cavity hits overburden is 452 m³, assuming exactly hemispherical cavity. And outflow channel volume is 2340 m³ (6 m height, 12 m width and 40 m length of outflow channel). Interestingly, though the volume of coal affected by UCG process at any time, for same operating conditions, is different for the phase-I and phase-II, resultant calorific value of exit gases remains almost similar in both the phases. Similarly, the rate of coal gasification remains almost same in both phases. Therefore the time required for completion of each phase should be proportional to the volume of coal to be consumed in that particular phase for similar operating conditions. Table 1 presents a comparison between UCG process and its

performance during phase-I and phase-II. This comparison also uses some of the results of parametric studies on these models, which is the topic of next paper in this series.

Table 1. Comparison between phase-I and phase-II of UCG

no.	Parameter	Phase-I	Phase-II
1	General description	Initial radial (vertical) growth of cavity till the cavity hits the overburden in initial tear-drop shape cavity	Growth of cavity in horizontal direction along the horizontal outflow channel, starts after the cavity hits the overburden
2	Time	For the coal of interest, time required for phase-I can be 15-20% of the total time.	For coal of interest, time required for phase-II can be 80-85% of the total time.
3	Calorific value (CV) and its fluctuations	Maximum among average CVs obtained is 172 kJ/mol. Because of spalling, CV fluctuates around the average. value by +-10 kJ/mol.	Maximum among the average CVs obtained is 172 kJ/mol. Because of spalling, CV fluctuates around the average value by +-4 kJ/mol.
		The maximum of average CVs obtained by simulations for phase-I and phase-II is almost same. This observation can be generalized for different coals if the spalling rate is substantial for the reactions to sustain in rubble.	
4	Un-reacted coal in cavity	Almost no coal remains un-reacted in phase-I cavity because the reactive gases have to pass through the rubble.	In outflow channel, flow of reactive gases can bypass the rubble while flowing parallel through the void. This creates the conditions of reduced temperatures in some compartments resulting in possibility of unconsumed coal.
6	Effect of spalling rate variation	Lower spalling rates i.e. lower than critical spalling rate, shows effect of spalling rate on exit gas quality. However, higher spalling rates results in same quality of exit gas, without any effect of variation in spalling rates.	Spalling affects the exit gas quality in similar way to phase-I, however effect of spalling rate/condition is observed at much lesser values of spalling rates as the exit gas quality is resultant of dynamics in several compartments.
7	Importance of accurate flow pattern determination	Flow patterns are important factors and exit gas quality is a strong function of gas flow rates and flow patterns.	Flow distribution between void and rubble zones does not affect the exit gas quality significantly because of more number of compartments. Large number of compartments provides a balancing effect.
8	Amount of coal affected per unit coal consumed for same CV at similar operating conditions	Area of roof exposed to hot rubble is limited and this reduces the amount of coal heated and affected. This results in less amount of coal getting affected per kg of coal consumed. (~1.8 kg coal affected/kg coal consumed)	Area of roof exposed to hot conditions in rubble is relatively huge which provides high rates of pyrolysis resulting in huge amount of coal getting affected per kg of coal consumed. (~4 kg coal affected/kg coal consumed)
	(Affected coal = coal with reduced density)		
10	Validation	Model is validated by comparing its predictions with results of laboratory	Model is validated by comparison between model predictions and laboratory scale

		scale micro-UCG experiments.	experiments with similar flow conditions.
--	--	------------------------------	-------------------------------------------

The time required for completion of different phases depends strongly on thickness of coal seam. If thickness of a coal seam is very less, time required for completion of phase-I will be less, whereas the phase-I will last longer in case of thick coal seams. Therefore both these models are important and there may be cases where only one of them is sufficient to achieve reliable predictions.

Comparison with field trials

In this section, model results are compared with few field trial results on different type of coals. Figure 10 shows the comparison of predicted CV of the exit gas with those observed during different field trials.

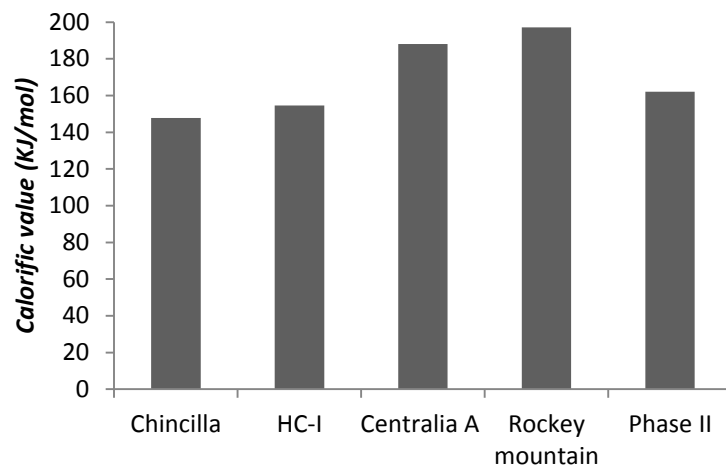


Figure 10. Comparison of calorific values (kJ/mol) of the product gas predicted by the present model for Vastan coal with different field trials (on dry basis)

The field trials selected are mostly the ones where a mixture of steam and oxygen is used as inlet gas¹⁷. Similar comparison between exit gas compositions predicted by the model and that observed during different field trials also provides a good agreement. This comparison is only to demonstrate that the predictions by the process model fall in line qualitatively with the UCG performances recorded in the worldwide field trials. No other inference can be drawn from these comparisons as the properties of coal and process conditions in each case are not very similar. However, for commercial applications of UCG, the comparison of the calorific value and compositions of product gas with that from different UCG trials may be

helpful as it can provide an initial indication of economic viability and possible end-use of the product gas.

Conclusion

Flow patterns in the outflow channel are non-ideal and hence a compartment model with parallel flow streams is proposed and solved for the outlet gas composition. The model proposed in this paper incorporates spalling, roof dynamics, transport processes and all important reactions including drying and pyrolysis. The model predicts that the calorific value of the exit gas fluctuates around an almost constant average for a long time till the volume of the void becomes higher than rubble volume. This observation goes well with most of the field trials showing fairly constant exit gas CV. Applicability of process model and reliability of its results depend on the accuracy of the model parameters like spalling condition, flow distribution in void and rubble, number of compartments in outflow channel and number of mixed reactors in rubble zone. These parameters are specific to the given coal seam and the operating conditions. The proposed model in the present work with appropriate parameters can be used for predicting and optimizing forward growth during several methods of UCG e.g. linked vertical wells (LVW), controlled retracting injection point (CRIP). Comparison between results of model and laboratory scale experiments shows an excellent match between experimental and model predictions of exit gas CV and time required for consumption of available coal. UCG performance predicted by this model is also in reasonably good agreement with the outcomes of different similar field trials thereby proving the suitability of the coal of interest for UCG. In addition, this paper also put forth the differences between phase-I and phase-II of UCG on parameters like spalling rate, amount of coal affected, gasification time and importance of flow pattern determination for Vastan coal. This comparison confirms the importance of our modeling approach of developing two different models for phase-I and II of UCG.

Notations

Acronyms

CRIP Controlled Retracting Ignition Point
CSTR Continuous Stirred Tank Reactor
DAE Differential-Algebraic Equation
LVW Linked vertical Wells
RTD Residence Time Distribution
UCG Underground Coal Gasification

WGS Water Gas Shift

Symbols

A_C	Area of cross-section (m^2)
A_{roof}	Area of roof surface (m^2) changes with time
C_g	Gas concentration ($kmol/m^3$)
C_p	Specific heat ($kJ/kmol/K$ for gas and $kJ/kg/K$ for solids)
D_{eff}	Effective Diffusivity (m^2/sec)
ΔH	Heat of reaction ($kJ/kmol$)
F_w	Rate of water influx ($kmol/sec$)
H	Enthalpy ($kJ/kmole$)
M	Molecular weight ($kg/kmol$)
V	Volume (m^3)
R_j	j^{th} reaction ($kmol/m^3/sec$)
T	Temperature (K)
a_{ij}	Stoichiometric coeff of i^{th} gas species in j^{th} reaction
$a_{s,ij}$	Stoichiometric coeff of i^{th} solid species in j^{th} reaction
h_T	Heat transfer coefficient in between gas and bed of particles ($kW/m^3/K$)
$h_{T_{\text{cav}}}$	Heat transfer coefficient from void to wall transfer ($kW/m^2/K$)
k_{eff}	Effective conductivity ($kW/m/K$)
$k_{y,\text{cav}}$	Mass transfer coefficient from void to wall transfer (m/sec)
t	Time (sec)
v_{df}	Velocity of drying front (m/sec)
ϵ_r	Radiation emissivity
ρ	Solid density (kg/m^3)
σ	Stefan boltzman constant ($kW/m^2/K^4$)
τ	Residence time in a zone (sec)
Φ	Porosity
v	Gas flow rate (m^3/sec)

Subscripts

g	Gas phase
s	Solid phase
c	Cross-section
w	Water influx or water
d	Drying
i	Species index
j	Reaction index
in	Inlet of a zone
void	Void zone in channel
roof	Cavity roof
vap	Vaporization
df	Drying front
spall	Conditions inside spalled rubble
T	Volume of total coal seam (at the end of wet zone)
l	Liquid phase

References

1. Aghalayam, P. *Underground Coal Gasification: A Clean Coal Technology*. In *Handbook on Combustion*; Wiley-VCH books, 2010; 257–275.
2. Samdani, G.; Aghalayam, P.; Ganesh, A.; Sapru, R. K.; Lohar, B. L.; Mahajani, S. M. A Process Model for Underground Coal Gasification- Part-I: Cavity Growth. Communicated with *Ind. Eng. Chem. Res.*
3. Shafirovich, E.; Varma, A. Underground Coal Gasification: A Brief Review of Current Status. *Ind. Eng. Chem. Res.* **2009**, 48, 7865.
4. Dinsmoor, B.; Galland, J.M.; Edgar, T.F. Modeling of cavity formation during underground coal gasification. *J. Petro. Tech.*, **1978**, 30, 695.
5. Chang, H.L. Process analysis and simulation of underground coal gasification flow model. 1984, PhD thesis. University of Texas at Austin.
6. van Batenburg, D.W.; Biezen, N.J.; Bruining, J., New channel model for underground gasification of thin, deep coal seams. *In Situ*, **1994**, 18, 419.
7. Coeme, A.; Pirard, J.P.; Mostade, M; Modeling of the chemical processes in a longwall face underground gasifier at great depth. *In Situ*, **1993**, 17, 83.
8. Kuyper, R.A.; Van Der Meer, Th.H.; Hoogendoorn, C.J. Turbulent natural convection flow due to combined buoyancy forces during underground gasification of thin coal layers. *Chemical Engineering Science*, **1994**, 49, 851.
9. Kreinin, E.V.; Shifrin, E.I. Mathematical modeling of the gas generation process in a coal reaction chamber. *J. Mining Sci.* **1995**, 31, 230.
10. Perkins, G. Numerical modelling of underground coal gasification and its application to Australian coal seam conditions. **2005**
<http://www.ac3.edu.au/edu/papers/perkinsg01.pdf>
11. Britten, J.A. Recession of a coal face exposed to a high temperature. *Int. J. Heat Mass Transfer*, **1986**, 29, 965.
12. Perkins, G.; Sahajwalla, V. Steady-State Model for Estimating Gas Production from Underground Coal Gasification. *Energy Fuels*, **2008**, 22, 3902.
13. Hill, R.W.; Thorsness, C.B.; Cena, R.J.; Aiman, W.R.; Stephens D.R. Results from the third LLL underground coals gasification projects: 1978 status. Proc. 4th Annual UCG Symp. Steamboat Springs, CO, July-1978.

14. Lyczkowski R.W.; Thorsness, C.B.; Cena, R.J. The use of tracers in laboratory and field tests of underground coal gasification and oil shale retorting. LLNL, UCRI-81252, 1978.
15. Bhaskaran S.; Samdani G.; Aghalayam P.; Ganesh A.; Singh R. P.; Sapru R. K.; Jain P. K.; Mahajani S. Experimental studies on spalling characteristics of Indian lignite coal in context of Underground coal gasification. Communicated to Fuel.
16. Samdani G. Mahajani S.M.; Ganesh A.; Aghalayam P.; Sapru R.K.; Lohar B.L. Importance of Spalling of Coal during the Cavity Modeling of Underground Coal Gasification (UCG) Reactor. 23rd International Symposium on Chemical Reaction Engineering (ISCRE-23). Bangkok, Thailand, September, 2014.
17. Perkins G. Mathematical modeling of underground coal gasification, 2005, PhD Thesis. University of New South Wales.